A miniaturized flexible frequency selective surface for dual band response

Durai Kanchana[1] (iD), Sankararajan Radha[1,2], Balakrishnapillai Suseela Sreeja[1] (iD) and Esakkimuthu Manikandan[2]

[1]Sri Sivasubramaniya Nadar College of Engineering, Chennai 603110, India and [2]School of SENSE, VIT Chennai campus, Chennai, India

Abstract

In this paper, a novel miniaturized and flexible dual band frequency selective surface (FSS) is presented. This FSS provides effective shielding in X-band and Ku- band, with a frequency response of 9.4 and 16.7 GHz, respectively. The proposed FSS provides 924 MHz bandwidth at X-band and 1.34 GHz bandwidth at Ku-band with an insertion loss of 20 dB. Moreover, the proposed design is polarization-independent and it provides stable frequency response at various angles of incidences for both transverse electric and transverse magnetic modes. More significantly, the proposed FSS analyzed the bandstop response of the selective frequency and also is suitable for conformal applications. A prototype of the proposed FSS is fabricated. The measured results and simulated results are good in agreement.

Introduction

Frequency selective surface (FSS) is a two-dimensional or three-dimensional periodical structure consisting of the metal patch (transmission coefficient) or slot structure (reflection coefficient). The fundamental characteristics of narrow bandwidth are used to achieve a sharp bandpass or bandstop response. It has been widely used in radomes, antenna reflectors to improve the gain, spatial filters, and electromagnetic shielding to control the transmission and reflection characteristics of the electromagnetic waves [1, 2]. The production of electronic devices is increasing day by day. Most recent and interesting research in electronics devices is developing flexible electronics like foldable tablets, laptop, and phones. At present, one of the most trending common approaches is to design an antenna and FSS in flexible materials. So, from that concept, the flexible or conformal FSS is designed with the help of polyimide (PI) material. The novelty of this paper is, by using a single layer flexible material, a miniaturized and dual band response is achieved and fabricated results have been reported and more significantly the bending analysis is also reported.

Many flexible FSS are reported in the literature. The performance of the FSS depends on the design and size of the unitcell element. Printed and flexible FSS illustrates in reference [3], the flexible FSS is printed on the plastic film using conductive and dielectric inks, and it provides tunable FSS with the help of the switching component. A miniaturized flexible FSS is designed using Roger 5880 material for X-band shielding application and it provides bandstop frequency response [4]. For conformal application, a serpentine-like FSS is printed on the PI material and also it provides stable responses for different angles of incidence [5]. A simple ring curvature FSS is printed on the flexible and transparent plastic substrate with a thickness of 1.6 mm using screen printing technology and it provides bandstop response at 12 GHz [6]. A paper [7] based on FSS structure is designed [8] and it coverts polarization from linear to circular polarized [9] at 7 GHz but the major drawback is, the quality of the material is poor. A convoluted ring-shaped FSS structure is designed for screening application at X-band frequency using a polyethylene terephthalate substrate but the fabrication process is very difficult because of using the silver nanoparticles [10].

In this paper, a simple theoretical analysis illustrates the mechanism of the proposed design, consisting of a modified double square loop (MDSL) element and it is printed on a single side of flexible PI material. This structure rejects both X- and Ku-band at center frequency of 9.4 and 16.7 GHz, respectively. Transmission characteristics of both transverse electric (TE) and transverse magnetic (TM) modes achieve the same frequency response, due to the symmetric design. Moreover, the proposed FSS design achieves stable frequency response for different angles of incidence upto 60° for both TE and TM modes. The simulated and measured results are the same for the proposed design.

Unitcell design

The topology of the proposed single layer FSS is illustrated in Fig. 1. The low-profile dual band FSS consisting of unitcell made of MDSL is printed on the flexible/conformable PI material with an overall thickness of 0.1 mm, dielectric constant of 3.5, and loss tangent value of 0.06. The
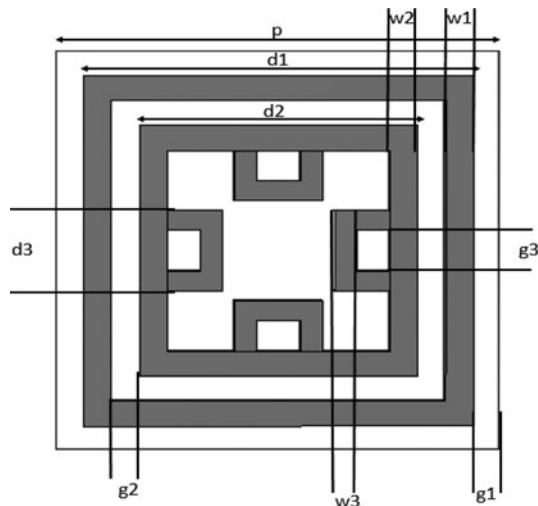
CAMBRIDGE
UNIVERSITY PRESS

Fig. 1. Unitcell element of the proposed design.

Fig. 2. Equivalent circuit of the modified double square loop structure.

proposed MDSL is evolved from the double square loop (DSL) design by convoluting the inner Square inwards bending c-shaped stub structure which is designed on all sides of the square loop.

MDSL equivalent circuit model

The equivalent circuit model (ECM) is used to analyze the proposed design of the MDSL FSS structure. This structure consists of DSL with C-stub which is designed to provide dual band frequency response.

Consider, the normalized inductive impedance expression of strip grating which were given by Marcuvitz as [11–15]

$$X_{TE} = F(p, w, \lambda)$$
$$= \frac{p \, \cos\theta}{\lambda}\left[\ln\operatorname{cosec}\left(\frac{w\Pi}{2p}\right) + G(p, w, \lambda, \Theta)\right], \quad (1)$$

where p represents the periodicity of the proposed structure, w is the width of the inductive strip (MDSL), λ is the wavelength, X_{TE}, the inductive impedance of TE mode, and $G(p, w, \lambda \, \Theta,)$ is the correction factor.

From the Babinet's duality condition, the susceptance for TM-incidence can be found

$$B_{TM} = F(p, w, \lambda)$$
$$= 4\frac{p \, \cos\Phi}{\lambda}\left[\ln\operatorname{cosec}\left(\frac{g\Pi}{2p}\right) + G(p, g, \lambda, \Phi)\right] \quad (2)$$

Equations (1) and (2) are valid only if $w \ll p$, $d \ll p$, and $p \ll \lambda$. Similarly, the inductance of the TM-incidence and the capacitance of the TE-incidence can be written as follows:

$$X_{TM} = F(p, w, \lambda)$$
$$= \frac{p \, \sec\theta}{\lambda}\left[\ln\operatorname{cosec}\left(\frac{w\Pi}{2p}\right) + G(p, w, \lambda, \Theta)\right], \quad (3)$$

$$B_{TE} = F(p, w, \lambda)$$
$$= 4\frac{p \, \sec\Phi}{\lambda}\left[\ln\operatorname{cosec}\left(\frac{g\Pi}{2p}\right) + G(p, g, \lambda, \Phi)\right] \quad (4)$$
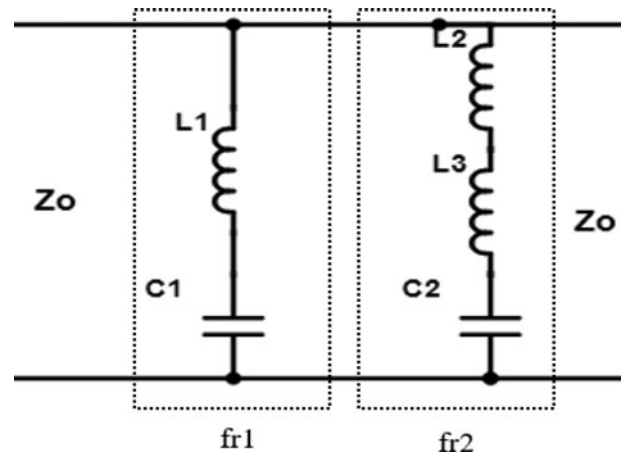
Here the G factor is neglected due to minor deviation occurrence. The given FSS structure is to change the response when the angle of incidence of the wave is changed and to avoid the grating lobes, equation (5) periodicity is related to the wavelength equation that is used in [16, 17].

$$p(1 + \sin\Theta) < \lambda \quad (5)$$

In general, the above equation for TE mode is also applicable for TM mode because of the square loop structure, the polarization-independent character is occurred and achieved the same response for TE and TM mode and for angle of incidence (Θ, Φ) can be used, respectively.

From the above basic equations, the proposed structure inductance and susceptance values are represented as,

$$X_{L1} = \frac{p}{d1} \, F(p, 2w1, \lambda1), \quad (6)$$

$$X_{L2} = \frac{p}{d2} \, F(p, 2w2, \lambda2), \quad (7)$$

$$B_{C1} = 4\frac{p}{d1} \, F(p, g1, \lambda1), \quad (8)$$

$$B_{C2} = 4\frac{p}{d2} F(p, g2, \lambda2). \quad (9)$$

In Fig. 2, the L_1 and C_1 are used for outer square loop structure and the frequency response is calculated using fr_1 value, and the inner square loop with C-stub FSS structure having series of combination of L_2, L_3, and C_2. The L_3 for C-stub is added as the inductance value and is used to achieve the desired frequency response. Multiple simulations have been done to find the L and C values using ADS tool. Since the thickness of the substrate is very small the effect of the transmission line is neglected. Where Z_{FSS}, the impedance of the proposed structure and the corresponding resonant frequency of fr_1 and fr_2 are calculated
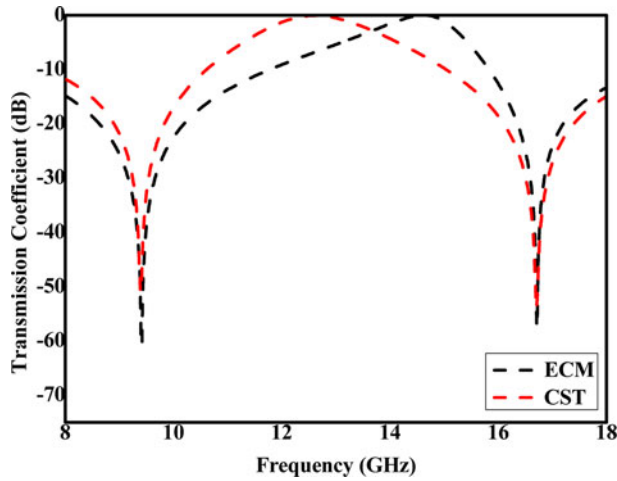
Fig. 3. Comparison of ECM result and simulation result.

Table 1. LC Values of the proposed design.

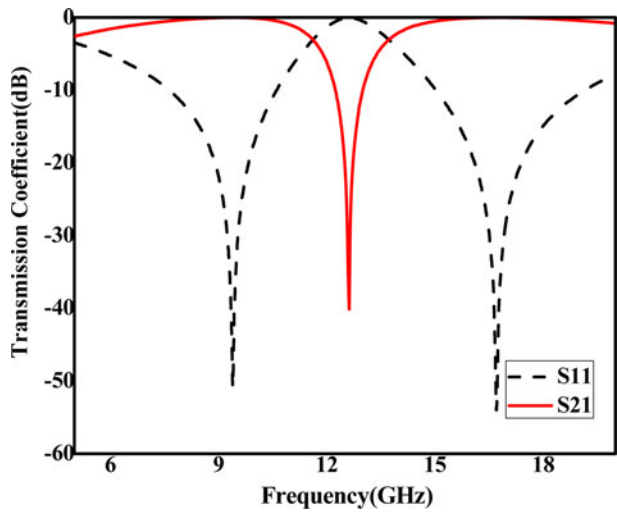| Parameter	L_1	C_1	L_2	L_3	C_2
Values	1.91 nH	0.15 pF	2.36 nH	1.27 nH	0.025 pF

Fig. 4. S-Parameters of the proposed FSS unitcell.

using the numerator of equation (11) equals to zero.

$$Z_{\text{FSS}} = \left[\frac{1 - \omega 2L1C1}{j\omega C1}\right] + \left[j\omega L2 + j\omega L3 + \frac{1}{j\omega C2}\right], \quad (10)$$

$$Z_{\text{FSS}} = \frac{1 - \omega 2L1C1}{j\omega C1} + \frac{1 - \omega 2C2(L2 + L3)}{j\omega C2}, \quad (11)$$

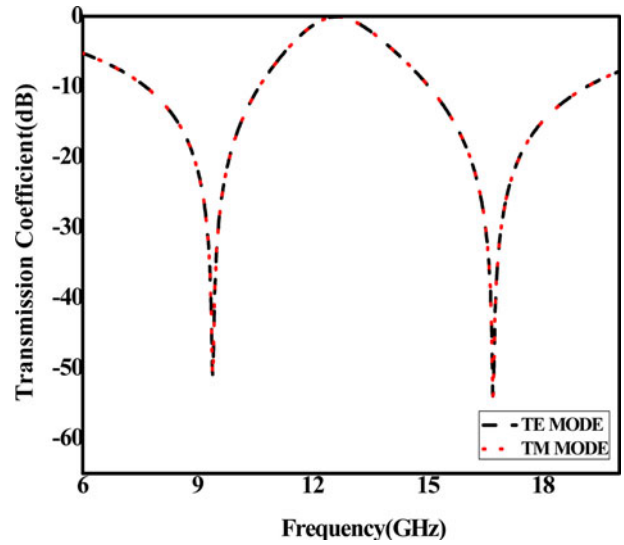$$fr_1 = \frac{1}{2\Pi\sqrt{L1C1}}, \quad (12)$$

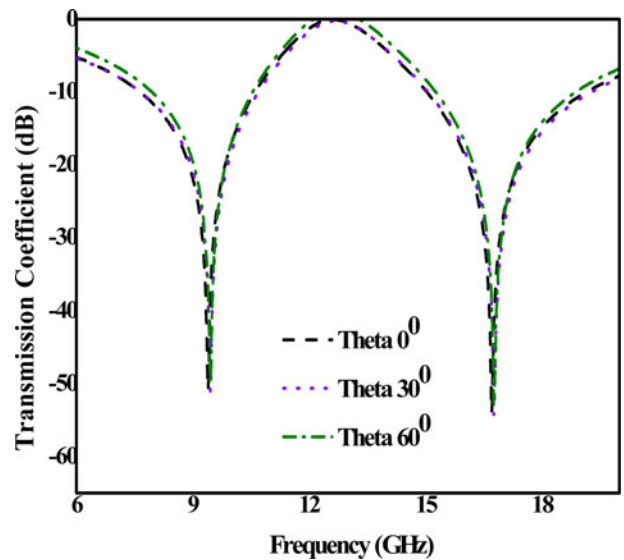Fig. 5. Transmission characteristics of both TE and TM mode.

Fig. 6. Effect of changing different angle of incidence on TE mode response.

$$fr_2 = \frac{1}{2\Pi} \sqrt{\frac{1}{(L2 + L3)C2}}. \quad (13)$$

Finally, the admittance of the MDSL design is calculated for more compact form in equation (14) by using the equivalent circuit seen in Fig. 2,

$$Y = j\left[\frac{B1}{1 - X1B1} + \frac{B2}{1 - B2(X2 + X3)}\right]. \quad (14)$$

The optimization parameter of the proposed structure is set as follows: $2.5 \leq p \leq 7.67$ mm, $1.3 \leq d1 \leq 6.0$ mm, $3.57 \leq d2 \leq 4.36$ mm, $2.6 \leq d3 \leq 4.16$ mm, $0.1 \leq w1 \leq 2.0$ mm, $0.1 \leq w2 \leq 2.0$ mm, $0.1 \leq w3 \leq 2.0$ mm, $0.2 \leq g1 \leq 2.26$ mm, $0.2 \leq g2 \leq 2.0$ mm, $0.02 \leq g3 \leq 0.6$ mm. The obtained parameters are $p = 5.4$ mm, $d1 = 5.0$ mm, $d2 = 4.2$ mm, $d3 = 3.8$ mm, $w1 = 0.4$ mm, $w2 = 0.4$ mm, $w3 = 0.4$ mm, $g1 = g2 = g3 = 0.4$ mm. The transmission
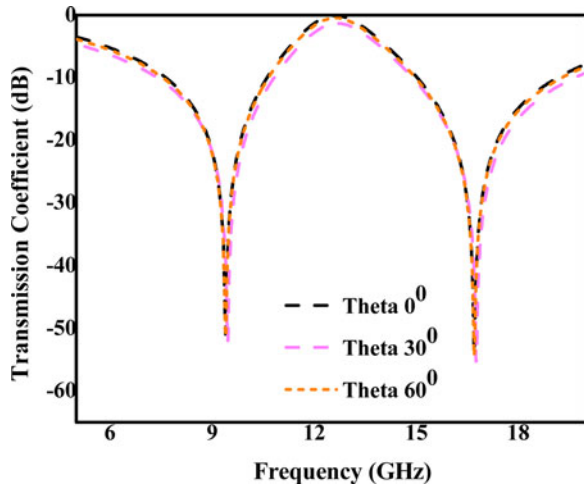
Fig. 7. Effect of changing different angle of incidence on TM mode response.

Table 2. Bandwidth response for TE and TM modes.

Different modes	Different angle of incidence for both frequency response		
	0°	30°	60°
TE MODE	0, 0	0, 16.88	9.44, 16.93
TM MODE	0, 0	9.38, 16.66	9.345, 16.69

Fig. 8. Effect of changing substrate material.

characteristics of both computed and optimized results are in good agreement and are shown in Fig. 3. The resonant frequencies of the simulated bandstop response achieved at 9.4 GHz and 16.7 GHz using CST tool and the measured result achieved 9.42 and 16.72 GHz using ADS tool. Table 1 represents the LC values of the proposed structure.

Simulation results

Using a commercially available CST microwave studio software, the proposed single layer PI material-based FSS is designed and simulated, and the simulation was done in frequency domain solver. A single layer PI substrate is used with a thickness of 0.1 mm and dielectric constant of 3.3. The transmission coefficient (bandstop) and reflection coefficient (band pass) of the proposed MDSL FSS simulation result are shown in Fig. 4. The transmission coefficient (S_{12}) result provides dual bandstop response at X-band 9.4 GHz and Ku-band 16.7 GHz at 20 dB attenuation and it provides 924 MHz and 1.34 GHz bandwidth, respectively. The corresponding reflection coefficient (S_{11}) provides band pass in transmission coefficient frequency response. Figure 5, inference the same frequency response for both TE and TM modes because of the identical unitcell design and it enables the polarization-independent characteristic. Thus, the proposed conformal FSS design provides dual band frequency response that is used for effective shielding applications.

Effect of changing angle of incidence

The performance of the proposed FSS under oblique incidence for TE and TM modes upto 60° angle of incidence is presented in Figs 6 and 7. C-Stub or shaped analyze are mainly used for angular
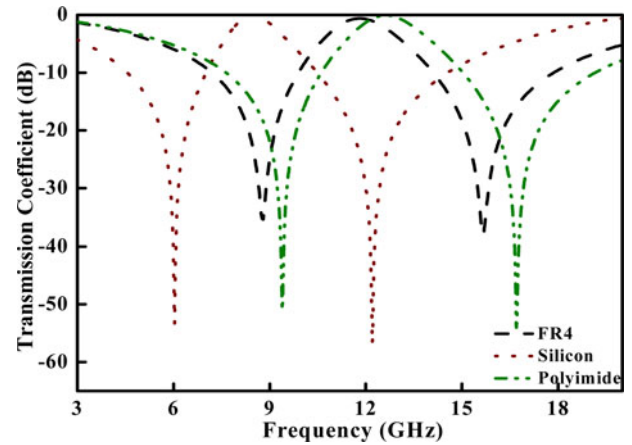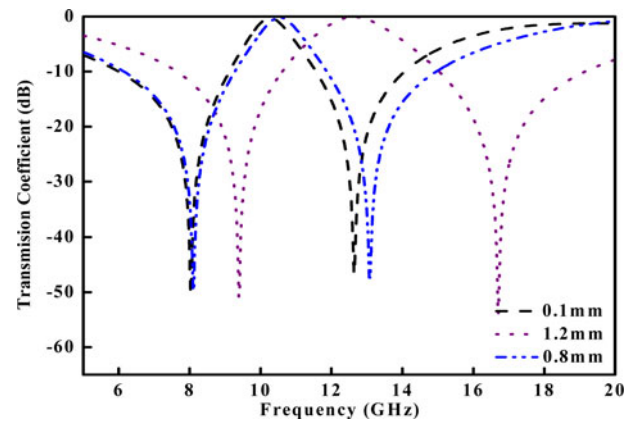

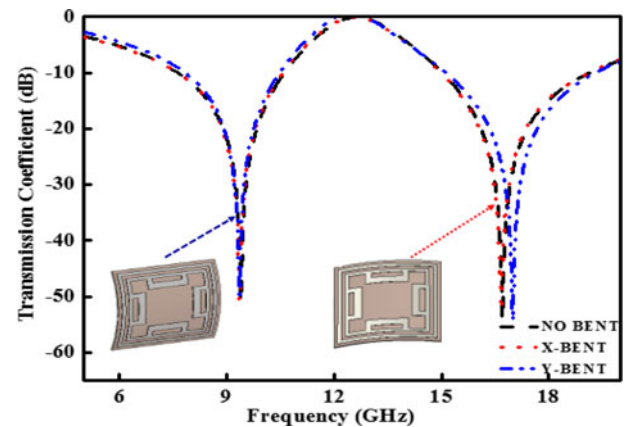Fig. 9. Effect of changing substrate thickness.

Fig. 10. Bending analysis for testing conformability.

stability [18]. It is observed that the bandstop response is changed depending on the propagation constant of TE and TM mode. In Fig. 6, the transmission coefficient of varying an angle of incidence upto 60° for TE Mode is shown, there is a minute frequency change that has occurred at 60° and the other angles are the same. In Fig. 7, the transmission coefficient of varying an incidence angle for TM mode is shown. It is observed that the frequency response is shifted little high at 30° and the other angles are the same. So, from the
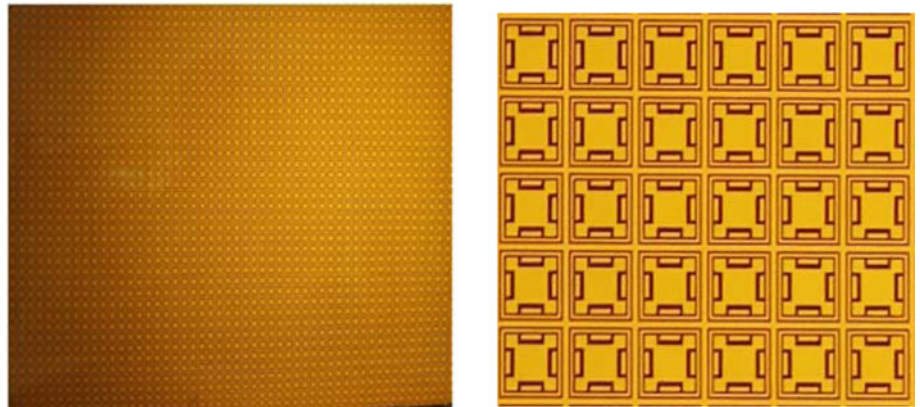
Fig. 11. (a) Fabricated flexible FSS prototype, (b) enlarged view.

effect of changing the incidence angles the frequency response is slightly changed but the changes are within the limits so the overall FSS is stable for both TE and TM modes and the comparison of bandwidth are detailed in Table 2.

Effect of changing materials

The performance of the proposed FSS is tested for different materials using three different materials which are chosen, FR4, Silicon, and PI material. In Fig. 8, the silicon substrate has a high dielectric constant (11.9) compared to others and the second highest is FR4 (4.3) and the final one is PI material (3.3). From Fig. 6, it is observed that the bandstop frequency is shifted towards the lower frequencies in both silicon and Fr4 material because of the dielectric constant. If the dielectric constant increases, the frequency will decrease. This is because of the electrical length "l" and dielectric constant "εeff" equation ($l \propto 1/\sqrt{\varepsilon eff}$). So, from this, the PI material achieves exact dual band frequency at X- and Ku-band response with high transmission coefficient.

Effect of changing substrate thickness

The parametric study has been done for the proposed design using the substrate thickness. By varying the thickness of the substrate, the frequency response will change accordingly. From Fig. 9, it is observed that the proposed design with 0.1 mm thickness has achieved high bandwidth and good transmission coefficient. While increasing the thickness of the substrate the frequency shifts to lower response. For conformal application, the lower substrate thickness is used.

Bending analysis

For various applications like parabolic reflector and aerospace, the conformal behavior is analyzed. To test the flexibility/conformability of the proposed design the bending analysis has been done with different scenarios using CST software and is shown in Fig. 10. When the curvature (bent) increases, the surface area of the unitcell also increases and the EM field exposes more. So, depending on the curvature the operating frequency of the bent analysis is varied and it is evident that the proposed FSS structure provides negligible shift at its operating frequencies for X-bent and Y-bent. So, the proposed design compared the results of *X* and *Y*-bent analysis with no bent results, hence it provides the same response. So, it is able to use for conformal applications.
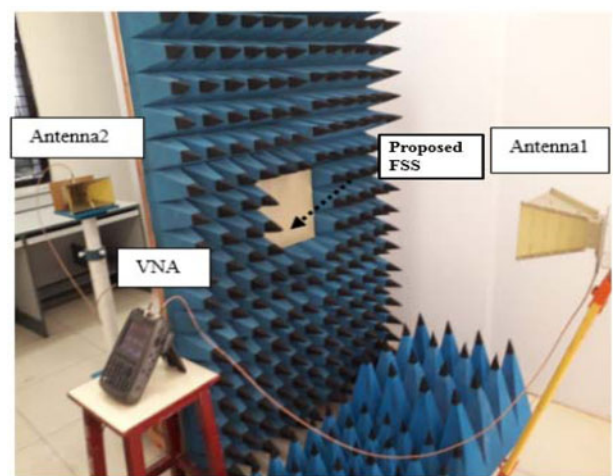
Fig. 12. Measurement setup for the proposed design.

Measurement setup

For the verification of the simulation results, the proposed design is fabricated and tested and the overall dimension of the fabricated prototype is 35cm × 35cm and is shown in Fig. 11. The fabricated prototype is tested using an experimental setup as shown in Fig. 12. The proposed FSS is fabricated on the flexible PI material with a thickness of 0.1 mm with 3.5 dielectric constant. The experimental setup consists of two pairs of horn antennas, one to measure the frequency between 1 and 12 GHz (JR-12) and the other to measure the frequency between 12 and 18 GHz (KU5086). Generally, the horn antenna used to transmit and receive the signal and the antennas connected through the Agilent technologies (VNA) N9917A which is used in-between the anechoic chamber stand is used to place the fabricated prototype and to avoid distortion. Initially, the measurement is carried without a fabricated prototype and then the measurement is carried with FSS prototype. Comparison of measured and simulation results are shown in Fig. 13.

From Figs 14 and 15, the measured results of a different angle of incidence for both TE and TM mode are shown. Little deviation occurs in frequency response for both TE and TM mode but it is an acceptable value. Due to the edge reflections and scattering of EM waves, a lack of smoothness is encountered during the measurements.
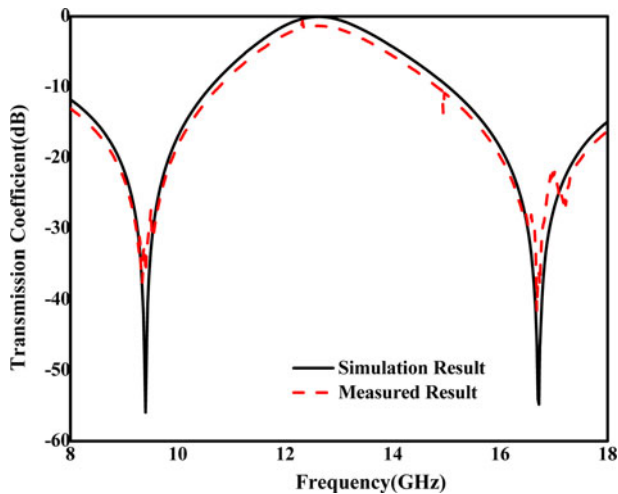
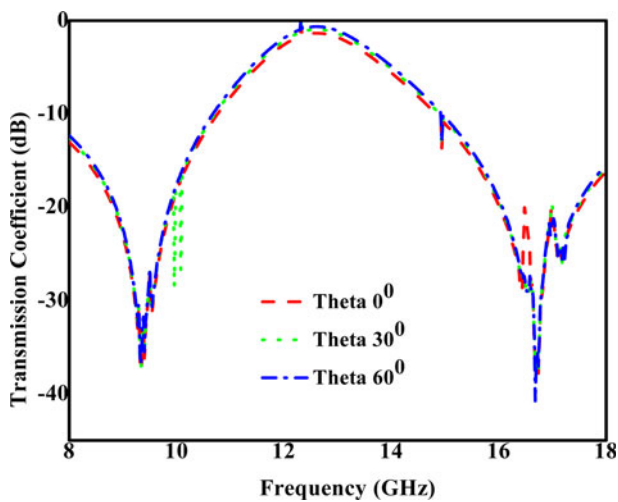**Fig. 13.** Comparison of simulation and measured result.

Fig. 14. Measurement results for different angle of incidence in TE mode response.
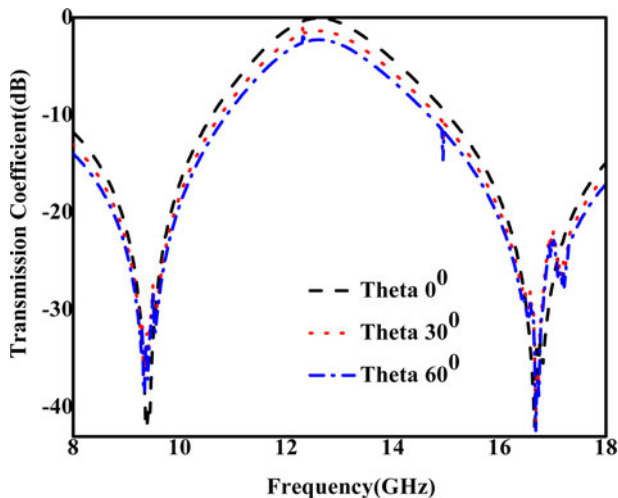

Fig. 15. Measurement results for different angle of incidence in TM mode response.

Conclusion

A thin and flexible-based FSS structure with dual stop band characteristic is proposed in this document. The proposed design provides a stable frequency response for both TE and TM modes under the various angle of incidence upto 60°. The proposed design verified the parameter effects of changing materials, electrical length, substrate thickness, and angles of incidence. A prototype of the fabricated measured results and simulation results are in good agreement. It provides dual band response with attenuation of 52 and 58dB, respectively. More significantly, the bending analysis is done and it verifies the suitability of conformal applications.

References

1. **Munk BA** (2000) *Frequency Selective Surfaces: Theory and Design*, 1st Edn. New York, NY, USA: Wiley.
2. **Munk BA** (2003) *Finite Antenna Arrays and FSS*. Hoboken, NJ, USA: Wiley.
3. **Haghzadeh M and Akyurtlu A** (2016) All-printed, flexible, reconfigurable frequency selective surfaces. *Journal of Applied Physics*, **120**, 184901. doi: 10.1063/1.4967169.
4. **Nauman M, Saleem R, Rashid AK and Shafique MF** (2016) A miniaturized flexible frequency selective surface for X-band applications. *IEEE Transactions on Electromagnetic Compatibility*, **58**, pp. 419–428. doi: 10.1109/TEMC.2015.2508503.
5. **Chen S, Pan T, Yan Z, Dai L, Peng Y, Gao M and Lin Y** (2019) Flexible serpentine like frequency selective surface for conformal applications with stable frequency response. *IEEE Antennas and Wireless Propagation Letters* **18**, 1477–1481. doi: 10.1109/LAWP.2019.2920369.
6. **Dewani AA, O'Keefe SG, Thiel DV and Galehdar A** (2017) Optically transparent frequency selective surfaces on flexible thin plastic substrates. *AIP Advances* **5**, 027107. doi: 10.1063/1.4907929.
7. **Lee S-H, Kim M-S, Kim J-K, Lim J-I and Hong I-P** (2018) Security paper design with frequency-selective structure for X-band electromagnetic detection system. *International Journal of Antennas and Propagation*, 1–8. doi: 10.1155/2018/9836937.
8. **Sivasamy R and Kanagasabai M** (2019) Design and fabrication of flexible FSS polarizer. *International Journal of RF and Microwave Computer-Aided Engineering*. doi:10.1002/mmce.22002.
9. **Mirza H, Hossain T Md, Soh PJ, Jamlos MF, Ramli MN, Hassan ES, Al-Hadi AA and Yan S** (2018) Single layered swastika-shaped flexible linear-to circular polarizer using textiles for S-band application. *International Journal of RF and Microwave Computer-Aided Engineering* **28**, e21463.
10. **Yong WY, Rahim SKA, Himdi M, Seman FC, Suong DL, Ramli MR and Elmobarak HA** (2018) Flexible convoluted ring shaped FSS for X-band screening application. *IEEE Access*, **6**, pp. 11657–11665. doi: 10.1109/ACCESS.2018.2804091.
11. **Marcuvitz N.** (1951) *Waveguide Handbook*. NewYork: McGraw-Hill.
12. **Sung GHH, Kevin S, Michael N and Allan W** (2006) A frequency selective wall for interference reduction in wireless indoor environments. *IEEE Antennas Propagation Magazine* **48**, 29–37.
13. **Langley RJ and Parker EA** (1982) Equivalent circuit model for arrays of square loops. *Electronics Letters* **18**, 294–296.
14. **Lee CK and Langley RJ** (1985) Equivalent-circuit models for frequency selective surfaces at oblique angles of incidence. *IEE Proc. H – Microwave Antennas Propagation* **132**, 395–399.
15. **Costa F, Monorchio A and Manara G** (2012) Efficient analysis of frequency selective surfaces by a simple equivalent-circuit model. *IEEE Antennas and Propagation Magazine* **54**, 35–48.
16. **Jha KR, Singh G and Jyoti R** (2012) A simple synthesis technique of single square-loop frequency selective surface. *Progress In Electromagnetics Research B* **45**, 165–185.
17. **Reed JA** (1997) *Frequency Selective Surfaces with Multiple Periodic Elements*. (Ph.D. dissertation). University of Texas at Dallas, USA.
18. **Parker EA and El Sheikh ANA** (1991) Convoluted array elements and reduced size unit cells for frequency-selective surfaces. *IEE Proceedings – H Microwave Antennas Propagation* **138**, 19–22.

D. Kanchana is a research scholar in the Department of Electronics and Communication Engineering at Sri Sivasubramaniya Nadar College of Engineering, Chennai, Tamil Nadu, India. She received her B.E. (ECE) in Sri Sairam Institute of Technology, Anna University, Chennai, Tamil Nadu, India in 2015 and completed her M.E. Communication systems in 2017. Her research interests are Frequency Selective Surfaces, Electromagnetic Shielding, and Microwave Engineering.

Dr. S. Radha is Professor and Head of the Department of ECE at Sri Sivasubramaniya Nadar College of Engineering, Chennai, Tamil Nadu, India. She has 24 years of teaching and 15 years of research experience in the area of Wireless Networks. She graduated in Electronics and Communication Engineering in 1989 from Madurai Kamraj University, Tamil Nadu, India. She obtained her Master degree in Applied Electronics with First Rank from Government College of Technology, Coimbatore, Tamil Nadu, India and Ph.D. degree from College of Engineering, Gunidy, Anna University, Chennai, Tamil Nadu, India.

Dr. B.S. Sreeja is an Associate Professor in the Department of ECE at Sri Sivasubramaniya Nadar College of Engineering, Chennai, Tamil Nadu, India. She has 14 years of teaching experience. She graduated in Electronics and Communication Engineering in 2002 from Bharathidasan University, Tamil Nadu, India and obtained Master of Engineering and Doctoral degrees from Satyabhama University, Chennai, Tamil Nadu, India. Her current research interests involve devices including MEMS, NEMS, and RF structures.

Dr. E. Manikandan is an Assistant Professor in the Department of ECE at B.S. Abdur Rahman Crescent Institute of Science and Engineering, Tamil Nadu, India. He has 4 years of teaching experience. He graduated in Electronics and Communication Engineering in 2010 from Anna University, Chennai and obtained Master of Engineering from Anna University, Chennai, Tamil Nadu, India. His current research interests involve devices including Terahertz Devices, Micromachining, Sensors, Nano- Electronics.